ELM-crash-induced RMP ELM suppression in DIII-D — lessons for CEMM

J.D. Callen, University of Wisconsin, Madison, WI 53706-1609

CEMM Meeting, San Jose, CA, October 30, 2016

Questions to be addressed:

1) How do applied $n = 2$ resonant magnetic perturbations (RMPs) suppress ELMs in recent DIII-D experiments.[1,2]

2) What are key elements of comprehensive model developed[3,4] **to describe and quantify the many stages in these experiments?**

3) How does an ELM crash precipitate bifurcation into an ELM suppressed state if the applied RMP is large enough?

4) Issues for CEMM $\Longrightarrow$ nonlinear forced magnetic reconnection.

[1] C. Paz-Soldan et al., "Observation of a Multimode Plasma Response and its Relationship to Density Pumpout and Edge-Localized Mode Suppression," Phys. Rev. Lett. **114**, 105001 (2015).

[2] R. Nazikian et al., "Pedestal Bifurcation and Resonant Field Penetration at the Threshold of Edge-Localized Mode Suppression in the DIII-D Tokamak," Phys. Rev. Lett. **114**, 105002 (2015).

[3] J.D. Callen, M.T. Beidler, N.M. Ferraro, C.C. Hegna, R.J. La Haye, R. Nazikian, C. Paz-Soldan, "Model of ELM suppression by RMPs in DIII-D," report UW-CPTC 16-3, July 2, 2016; paper and poster P5.0030 at EPS 43rd Conference of Plasma Physics, Leuven, Belgium, July 4–8, 2016.

[4] J.D. Callen, R. Nazikian, C. Paz-Soldan, N.M. Ferraro, M.T. Beidler, C.C. Hegna and R.J. La Haye, "Model of $n = 2$ RMP ELM suppression in DIII-D," draft report UW-CPTC report 16-4 prepared for submission to Plasma Physics and Controlled Fusion, currently undergoing DIII-D review.

Key Elements Of This Novel Model Are Different

- **Special characteristics of these $n = 2$ DIII-D experiments:[1,2]**

  RMP strength is slowly increased through threshold,
  rational surfaces are well separated, and
  only the 8/2 RMP penetrates.

- **$\omega_E \to 0$ is caused by ELM crash, not initiator of ELM suppression**

- **ELM crash causes reconnection, mode-locking and seed island**

- **RMP drive must be sufficient for island width to grow in MRE**

- **Electron flow, flutter transport and collisionality effects intertwined**

DIII-D Pedestals Can Bifurcate Into ELM Suppression[1,2]

- **Notes on Fig. 1 at right:**
  1) Green bands show ELM suppression.
  2) Red asterisks * highlight key responses to be discussed.
  3) Time slices to be described are
     $t_0 = 4307$ ms, minimum applied $|\delta B_\theta|$,
     $t_2 = 4701$ ms, just before suppression,
     $t_3 = 4781$ ms, during suppression.

- **When upper/lower $n = 2$ I-coil phasing produces maximum HFS-measured $|\delta B_\theta|$ at $t \gtrsim 3.7, 4.7$ s, ELMs are suppressed and abruptly**
  a) extra* $n=2$ tearing-type[1] $|\delta B_\theta|$ occurs,
  b) edge carbon tor. flow V_{Ct} increases,*
  c) electron density $n_{e,\mathrm{ped}}$ and temperature $T_{e,\mathrm{ped}}$ are reduced a bit.*

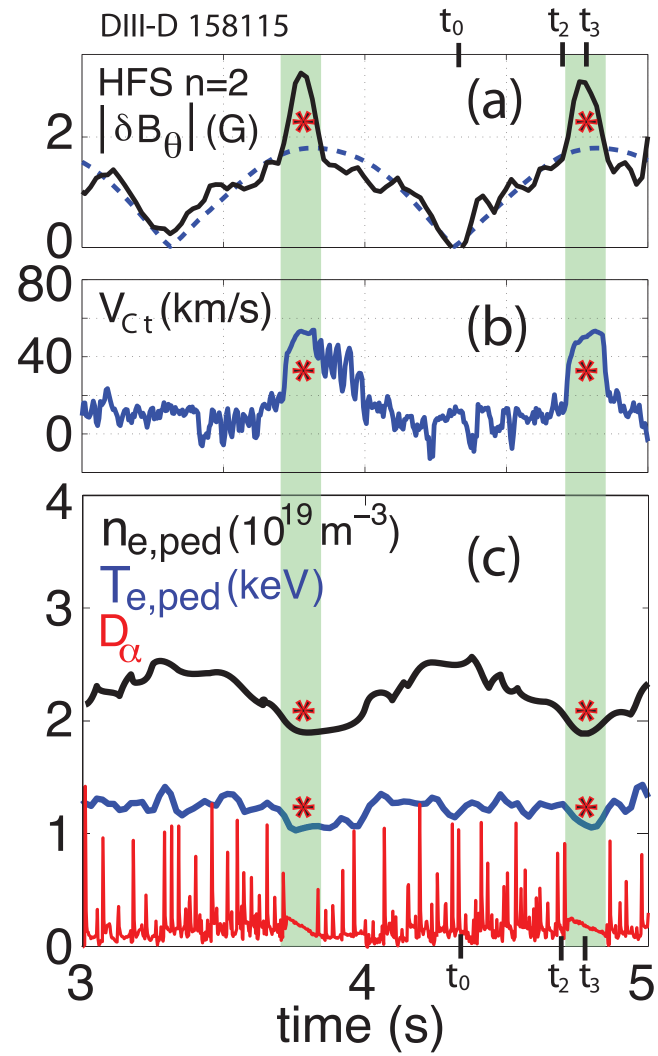

Figure 1: (a) varying the applied $|\delta B_\theta|$ changes (b),(c) pedestal parameters.[1,2]

ELM Crash Precipitates Bifurcation In δB_θ and V_{Ct}

- At $\boxed{t \gtrsim 4705 \text{ ms} > t_2}$

  an ELM crash occurs,

  after which the high-field-side (HFS) measured δB_θ increases abruptly* ($\lesssim$ ms?)

  and the CER-inferred ($\Delta t \simeq 5$ ms) edge carbon flow begins* to increase.

- On longer time scales:

  the extra* δB_θ continues growing** up to t_3,

  carbon tor. flow speed (V_{Ct}) also grows** up to t_3, but

  pedestal bifurcates[2] back to ELMing state at 4860 ms as RMP gets smaller.

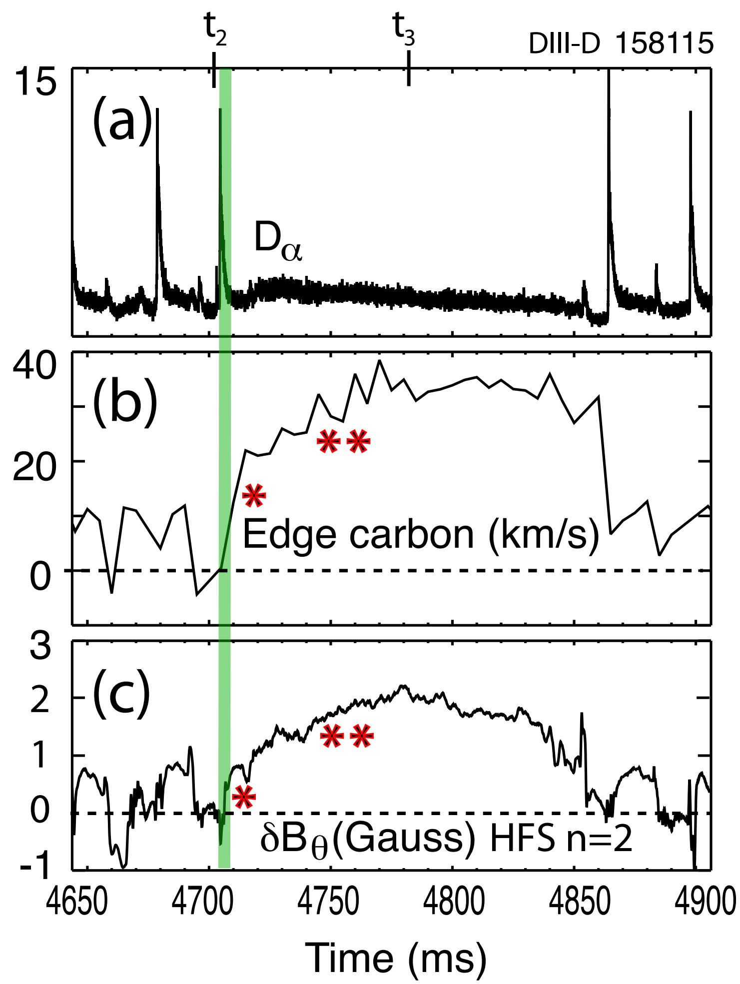

Figure 2: **Medium time scale of the bifurcation induced by ELM crash at 4705 ms, which occurs for the largest externally applied RMP, δB_θ.**

Profiles Are Different At $t_2 = 4701$ ms And $t_3 = 4781$ ms

- **Profiles are shown at two key time slices:**[2]
  at $t_2 = 4701$ ms, in ELMing "equilibrium" before suppression,
  at $t_3 = 4781$ ms, in saturated state during ELM suppression.

- **During suppression**

  (a) Thomson scatt. T_e, n_e gradients are reduced at the pedestal top ($0.9 < \Psi_N < 0.95$)

  flow frequencies (b) ω_E and (c) $\omega_{\perp e}$ are reduced at $q = 8/2 = 4$ surface,

  (e) resonant magnetic perturbations B_{mn} are flow screened except at 8/2 rational surface.

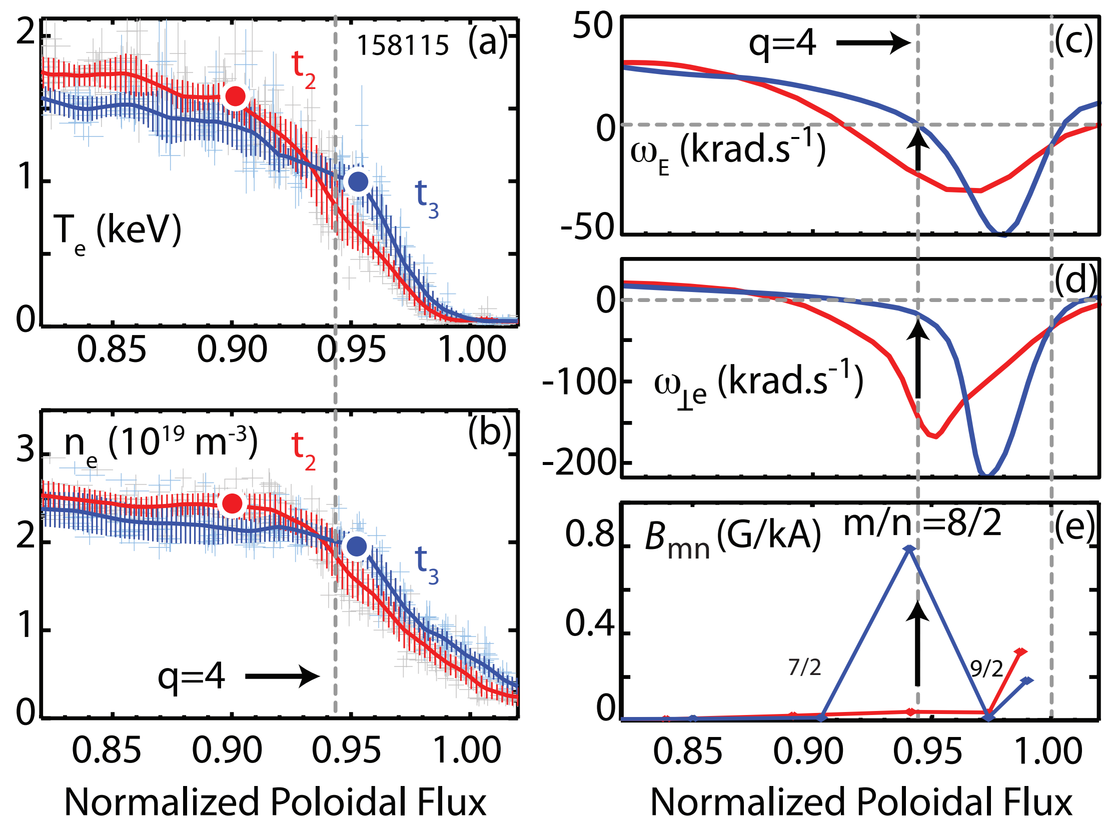

Figure 3: **Profiles before, during ELM suppression.**

Forced Magnetic Reconnection Theory Provides Context

- **When 3-D RMPs are applied to an axisymmetric tokamak plasma, two states are possible at $q = m/n$ rational surfaces:**
  - A) high slip state — RMPs are flow screened with little reconnection, or
  - B) low slip state — little flow screening and significant RMP field penetration occurs there, which induces a tearing-type (magnetic island) response.

- **States and bifurcations between them are described by forced magnetic reconnection (FMR) theory — slab,[5] cylinder,[6,7] tokamak.[8]**

- **Flow screening: In ELMing "equilibrium," RMPs are strongly flow screened at rational surfaces $q(\rho_{m/n}) \equiv m/n$ by a factor ($\tau_\delta \simeq 0.014$ s)**

$$f_{\rm scr} \equiv \frac{B_{mn}(\rho_{m/n})}{B_{mn}^{\rm vac}} \simeq \left| \frac{\rho_{m/n}\Delta'_{{\rm RMP}\, m/n}}{\rho_{m/n}\Delta'_{m/n} - in\Omega_e^\alpha \tau_\delta} \right| \sim \left| \frac{m}{-in\Omega_e^\alpha \tau_\delta} \right| \lesssim 0.04, \text{ at flow-screened surfaces.}$$

- **Relevant electron flow frequency is[8] (at rational surfaces[4] $\Omega_e^\alpha \to \omega_E$)**

$$\Omega_e^\alpha \equiv \omega_{\perp e} + \frac{0.71}{e}\frac{dT_e}{d\psi_{\rm p}}, \quad \omega_{\perp e} \equiv \omega_E + \omega_{*e}, \quad \omega_E \equiv -\frac{d\Phi_0}{d\psi_{\rm p}} = \frac{E_\rho}{RB_{\rm p}}, \quad \omega_{*e} \equiv \frac{1}{n_e e}\frac{dp_e}{d\psi_{\rm p}}.$$

---

[5] T.S. Hahm and R.M. Kulsrud, "Forced magnetic reconnection," Phys. Fluids **28**, 2412 (1985).
[6] R. Fitzpatrick, "Bifurcated states of a rotating tokamak plasma in the presence of a static error-field," Phys. Plasmas **5**, 3325 (1998).
[7] A.J. Cole and R. Fitzpatrick, "Drift-magnetohyrodynamical model of error-field penetration in tokamak plasmas," Phys. Plasmas **13**, 032503 (2006).
[8] J.D. Callen, C.C. Hegna, M.T. Beidler, "Forced magnetic reconnection in tokamak plasmas," to be published.

Modeled Resonant B_{mn} Are Flow Screened Except $m = 8$

- (a) at $t_2 = 4701$ ms,
  before suppression

  B_{mn} are flow-screened with
  $f_{\rm scr} \equiv B_{mn}(\rho_{m/n})/B_{mn}^{\rm vac} \lesssim 0.04$.

- (b) at $t_2 = 4781$ ms,
  during suppression

  most B_{mn} are flow-screened,
  but $B_{82}(\rho_{8/2})$ is not since
  $f_{\rm scr} \simeq 0.8$ at $8/2$ surface.

- Kink responses occur

  inward of the rational surfaces where $q < m/n$, and

  increase B_{mn} at top of pedestal ($0.9 < \rho_{\rm N} < 0.96$) — important for flutter transport $\propto B_{mn}(\rho)^2$.

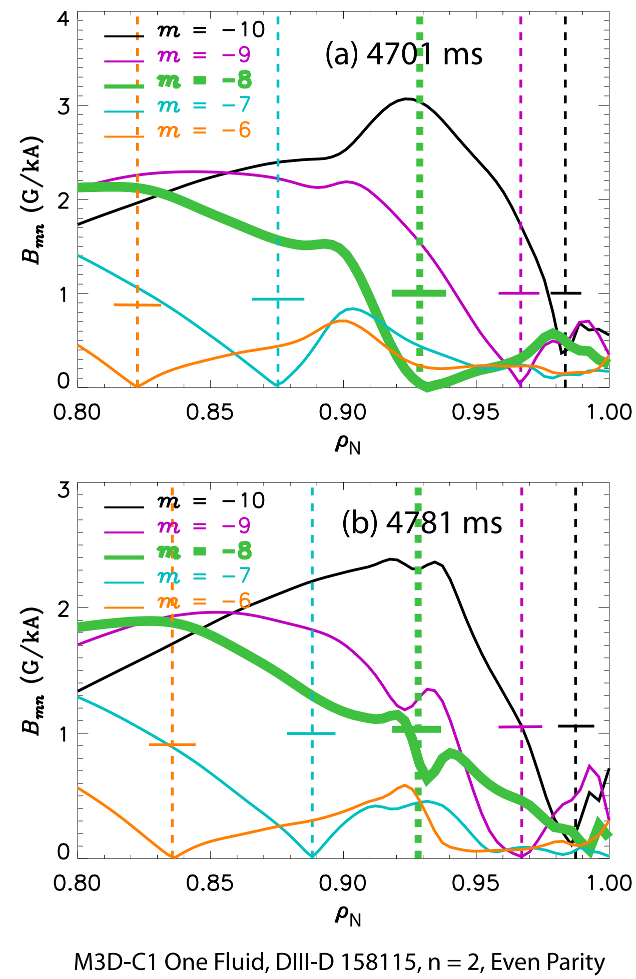

Figure 4: **Radial variation of RMP-induced perturbations $B_{mn}(\rho_{\rm N})$ from M3D-C^1. Bars show vacuum field strengths at each rational surface.**

Magnetic Field Models, Island Structures Are Different

- **Model used for B_{mn} is:**

  $$B_{mn} \equiv B_{mn}^{\rm vac}\sqrt{f_{\rm scr}^2 + x^2/L_{\delta B_\pm}^2},$$

  $B_{mn}^{\rm vac} \simeq 4.1$ G, $\delta_\eta \simeq 0.14$ cm,

  (a) at $t_2 = 4701$ ms,
  before suppression,
  high slip state with
  strong flow screening,
  island $w_{\rm hs} \simeq 0.5$ cm $\gtrsim 2\delta_\eta$,

  (b) at $t_2 = 4781$ ms,
  during suppression,
  low slip state with
  little flow screening,
  island $w_{\rm ls} \simeq 2.2$ cm $\gg 2\delta_\eta$.

- **Adjacent m/n surfaces are at domain edges.**

- **$\vec{B}$ flutters radially.**

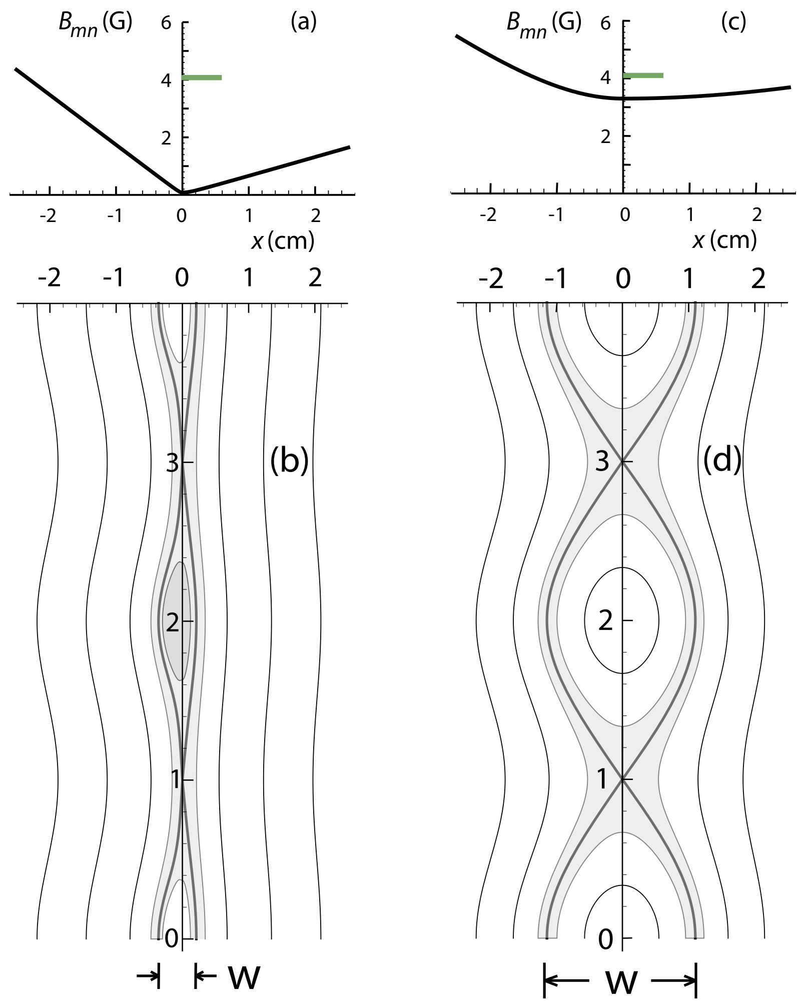

Figure 5: Modeled RMP, fields near 8/2 surface: (a),(b) before and (c),(d) during ELM suppression.

What Causes Bifurcation Into ELM Suppressed State?

- **Up to now the high and low slip states before and during ELM suppression are well separated in time and discussed separately.**

- **Next question is: what dynamical processes cause bifurcation?**

- **Next few viewgraphs describe**

  shorter time scale dynamics around 4705 ms ELM crash,

  theory of ELM-crash-induced RMP penetration & mode locking,

  growth of width of magnetic island during ELM suppression.

δB_θ Changes Precede Those In Carbon; Both Bifurcate

- **Many stages are involved:**

  4704.5–4705.5 ms: ELM at $\delta t \simeq 0$ causes $n=2$ $|\delta B_\theta|$ to increase* about 1.2 G,

  $\delta t \simeq$ 1–5 ms: residual $|\delta B_\theta|$ induced by ELM produces a seed island $w_{seed} \propto |\delta B_\theta|^{1/2}$,

  $\delta t \simeq$ 2–10: carbon rotation V_{Ct} at $\Psi_N \simeq 0.97$ increases monotonically* for largest RMP,

  $\delta t \simeq$ 5–12: $|\delta B_\theta|, V_{Ct}$ both bifurcate — they grow for largest RMP, decay for smallest RMP.**

  $\delta t \simeq$ 12–25: $|\delta B_\theta|$ grows more $\Longrightarrow$ growing island width $w \propto |\delta B_\theta|^{1/2}$.**

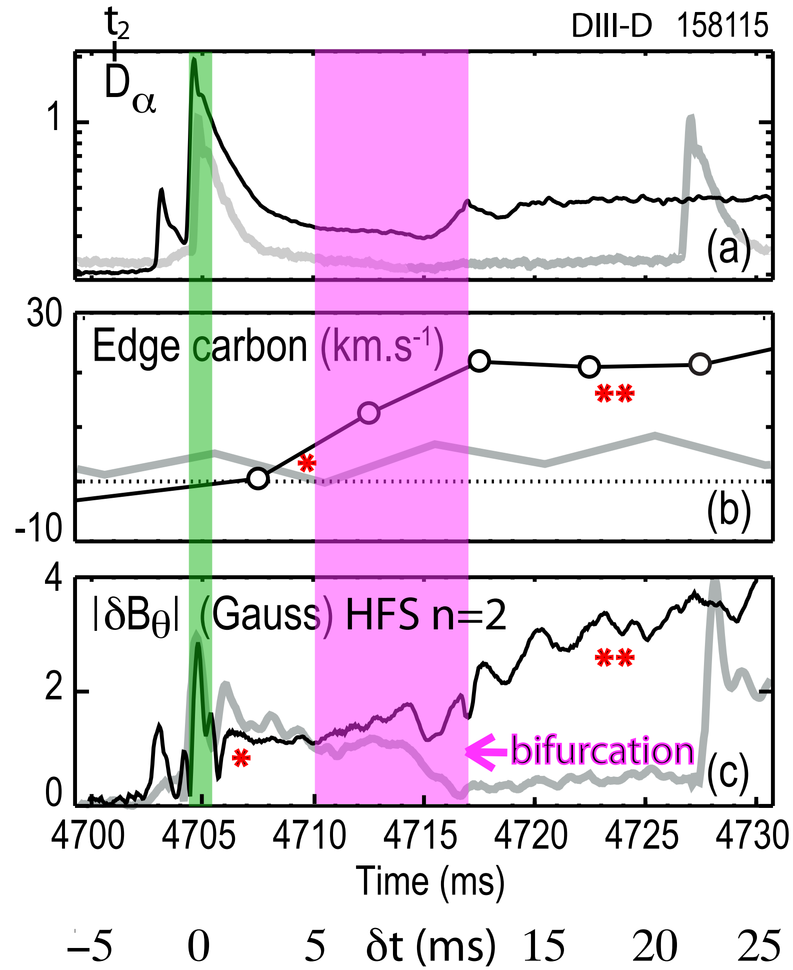

Figure 6: **Shortest time scale of bifurcation induced by ELM at 4705 ms for largest RMP. Gray lines are for smallest RMP with ELM at $t_0 = 4307$ ms.**

Change In Toroidal Angle Phase Indicates Mode Locking

- **During the ELM at 4704.5–4705.5 ms:**

  the ∼ linear increase of the Toroidal Angle with time implies $|\delta B_\theta|$ frequency of

  $$\omega_t^{res} \equiv \frac{\Delta(\text{Toroidal Angle})}{\Delta t} \simeq 2\times 10^3 \text{ rad/s} \sim \vec{\nabla}\zeta\cdot\frac{\vec{E}_0\times\vec{B}_0}{B_0^2}.$$

- **After 4706 ms ($\delta t \simeq 1$ ms) toroidal phase transitions**

  to $\omega_t^{res} \to 0$ state which implies $|\delta B_\theta|$ locks to RMP,

  and remains "mode-locked" to the lab frame as $|\delta B_\theta|$ bifurcates and continues to grow.**

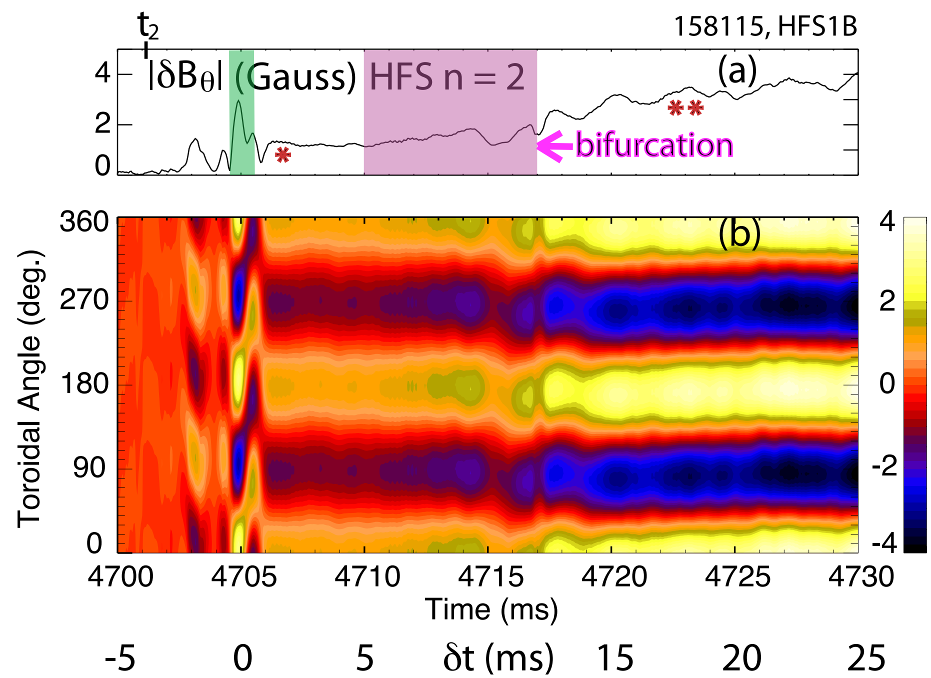

Figure 7: **Shortest time scale of (a) bifurcation during $\delta t \simeq 5$–12 ms induced by ELM at $\delta t \simeq 0$ (4705 ms) and (b) Toroidal Angle phase of the $n = 2$ $|\delta B_\theta|$ for largest RMP.**

Theory Of Reconnection, Mode Locking During ELM Crash

- FMR theory[9] is adapted to predict[4] growth of resonant field $B_{mn}^{\rm res}$ in response to ideal MHD magnetic perturbation $B_{82}^{\rm ELM} \simeq 3$ G:

$$|B_{82}^{\rm res}| \simeq \frac{\tau_{\rm FKR}}{\tau_{\rm SP}} C_{\rm ELM}\, B_{82}^{\rm ELM} \simeq 1.2 \text{ G}, \quad C_{\rm ELM} \simeq (\rho_{8/2}\Delta'_{\rm RMP\,8/2})^{3/2} \frac{\rm w_{ELM}}{4\rho_{8/2}} \simeq 0.95,$$

which implies a seed island width of $\mathrm{w_{seed}} \equiv 4\left[\frac{L_{\rm sh}}{k_\theta}\frac{B_{82}^{\rm res}}{B_{\rm t0}}\right]^{1/2} \simeq 1.3$ cm.

- Resistivity causes reconnected field $B_{82}^{\rm res}$ to induce a parallel current and consequently poloidal torque[4,8] on plasma $\tau_{e\theta} \propto \delta J_\parallel^{\rm res} B_{82}^{\rm res}$.

- Balancing $\tau_{e\theta}$ and $\tau_{i\theta}$ in equilibrium poloidal torque balance yields:[10]

$$E_\rho(\rho_{8/2}, t) = \frac{E_\rho^{\rm sym}}{\kappa(t)+1}, \quad \kappa(t) \equiv \frac{n_e T_i}{n_i T_e}\frac{D_{et}^{\rm flutt}}{D_i^{na}} \gg 1, \quad D_{et}^{\rm flutt}(\rho_{8/2}, t) \propto \left[\tfrac{\delta t}{\tau_{\rm FKR}}\right]^2 [B_{82}^{\rm res}]^2,$$

which forces $E_\rho(\rho_{8/2}) \sim \omega_E \nearrow 0$ in $\delta t \leq \tau_{\rm FKR} \simeq 0.4$ ms $\Longrightarrow$ mode-locked state.

---

[9] C.C. Hegna, J.D. Callen and R.J. LaHaye, "Dynamics of seed island magnetic island formation due to geometrically coupled perturbations," Phys. Plasmas **6**, 130 (1999).

[10] J.D. Callen, C.C. Hegna and A.J. Cole, "Magnetic-flutter-induced pedestal plasma transport," Nucl. Fusion **53**, 113015 (2013).

Initial $\delta t \simeq 1$–5 ms Tearing Response Stage Is Transient

- **The 4706–4710 ms stage in Figs. 6, 7 is a transient stage in which**
  1) **ballooning-type $n = 2$ P-B induced LFS observed δB_θ decays in ~ 3 ms,**
  2) **flutter transport radially diffuses δ_η layer responses over $\delta\rho_{\rm trans} \sim 2$ cm,**
  3) **neoclassical ion poloidal flow is damped to its equilibrium in $\tau_{ii} \sim 3$ ms,**
  4) **toroidal carbon ion flow $V_{\rm Ct}$ outside δ_η layer increases in response to $E_\rho \nearrow 0$ at 8/2 rational surface and $D_i^{\rm sym} \sim \mu_{i\perp}$ radial diffusion away from it,**
  5) **but the tearing-type magnetic perturbation δB_θ remains about constant.**

- **After these transient effects decay**
  1) **δB_θ remains locked to the stationary RMP frame (i.e., $\omega_{\rm t}^{\rm res} = 0$), and**
  2) **the overall toroidal plasma torque balance[11] becomes applicable,**
  3) **further growth of w $>$ w$_{\rm seed} \propto [B_{82}^{\rm res}]^{1/2}$ is governed by nonlinear MRE.[12]**

---

[11] J.D. Callen, A.J. Cole and C.C. Hegna, "Toroidal flow and radial particle flux in tokamak plasmas," Phys. Plasmas **16**, 082504 (2009); Erratum **20**, 069901 (2013)

[12] P.H. Rutherford, "Nonlinear growth of the tearing mode," Phys. Fluids **16**, 1903 (1973).

RMP-Driven MRE Indicates Narrow Range For w Growth

- **Modified Rutherford equation (MRE)[11] for 158115 parameters[1,2] is**

$$\dot{\mathrm{w}} \equiv \frac{\partial \mathrm{w}}{\partial t} = \frac{\eta_{\parallel}^{nc}}{\mu_0}\left[\Delta'_{8/2} + \Delta'_{\mathrm{RMP}}\frac{\mathrm{w}_{\mathrm{vac}}^2}{\mathrm{w}^2} - \frac{\mathrm{w}_{\mathrm{pol}}^3}{\rho_{8/2}\,\mathrm{w}^3}\right], \quad \mathrm{w}_{\mathrm{vac}} \simeq 2.4\ \mathrm{cm}, \quad \mathrm{w}_{\mathrm{pol}} \simeq 1.9\,\varrho_i q/\sqrt{\epsilon} \simeq 5.4\ \mathrm{cm}.$$

- **Parameters:**

  tearing stability $\rho_{8/2}\Delta'_{8/2} \simeq -16$,

  $\overline{\delta J_{\parallel\,8/2}}$ is induced by RMP (increased by kinking, $J_{\parallel \mathrm{bs}}$) $\rho_{8/2}\Delta'_{\mathrm{RMP}\,8/2} \simeq 26.4$.

- **For growth need $\dot{\mathrm{w}} > 0$:**

  $\mathrm{w}_{\mathrm{vac}} > \mathrm{w}_{\mathrm{vac}}^{\mathrm{crit}} \simeq 2.3\,\mathrm{cm}$ where

  $$\mathrm{w}_{\mathrm{vac}}^{\mathrm{crit}} \equiv \mathrm{w}_{\mathrm{pol}}\frac{[\,(27/4)\,|\rho_{8/2}\Delta'_{8/2}|\,]^{1/6}}{[\rho_{8/2}\Delta'_{\mathrm{RMP}\,8/2}]^{1/2}},$$

  and $\mathrm{w}_{\mathrm{seed}} > \mathrm{w}_{\mathrm{min}} \simeq 1.28$ cm.

- **max{$\dot{\mathrm{w}}$} growth time:**

  $\tau_{\mathrm{w}}\big|_{\max\{\dot{\mathrm{w}}\}} \equiv \frac{\mathrm{w}}{\max\{\dot{\mathrm{w}}\}}$ $\simeq$ 20 ms (see ** Fig. 6).

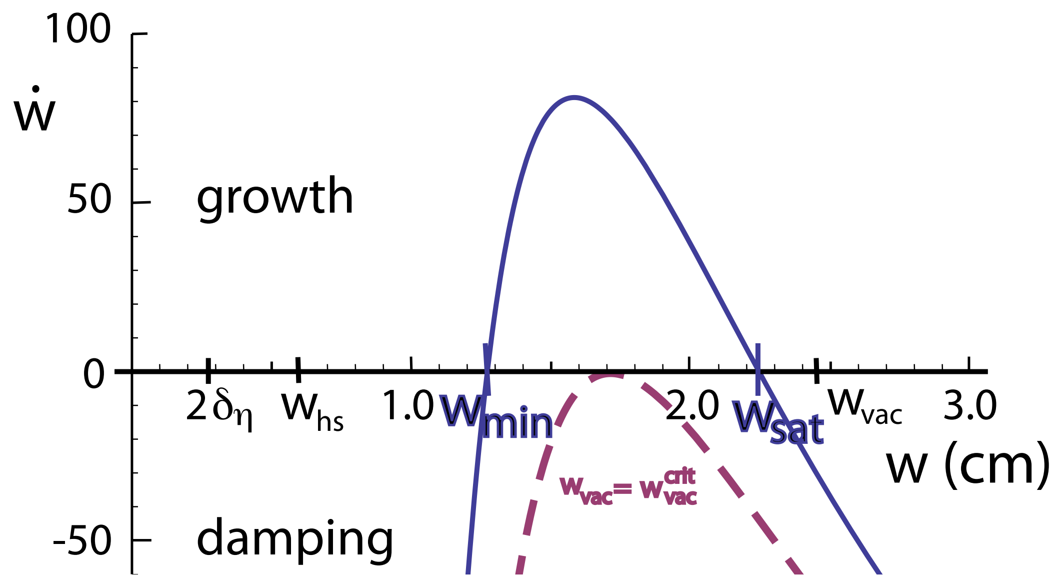

Figure 8: **Growth of magnetic island ($\dot{\mathrm{w}} > 0$) occurs for $\mathrm{w}_{\mathrm{min}} < \mathrm{w} < \mathrm{w}_{\mathrm{sat}}$. Island decays if $\mathrm{w}_{\mathrm{seed}} < \mathrm{w}_{\mathrm{min}}$ because of $\mathrm{w}_{\mathrm{pol}}$ ion polarization current effects and $\mathrm{w} > \mathrm{w}_{\mathrm{sat}}$ due to negative tearing mode stability index $\Delta'_{8/2} < 0$.**

Magnetic Flutter Transport Plays Important Roles

- **Magnetic flutter transport processes have already been used:**

  1) flutter transport flattens T_e, n_e profiles in resistive layer $\delta_\eta \simeq 0.14$ cm around the rational surfaces, which causes $\Omega_e^\alpha \simeq \omega_{\perp e} \to \omega_E$ there, without affecting the T_e and n_e profiles outside these narrow layers — justifies use of one-fluid M3D-C1 modeling for B_{mn} spectra?

  2) flutter diffusivity $D_{et}^{\text{flutt}}(\rho_{8/2})$ must be large compared to non-ambipolar ion D_i^{na} to force $E_\rho \nearrow 0$ to produce mode locking during ELM crash; but D_{et}^{flutt} is smaller by $(\nu_{e\,\text{eff}}/n\Omega_e^\alpha)^2$ for large $\Omega_e^\alpha \simeq \omega_{\perp e}$ electron flows.

- **Because $\lambda_{e\,\text{eff}} \lesssim L_{\parallel\,\text{eff}}$, T_e, n_e profiles don't follow island topology, flutter transport model is used to estimate their diffusivities.**

- **Flutter transport model[4,10] predicts:**

  1) pedestal top $\chi_e^{\text{flutt}} \simeq 1.4\,\text{m}^2/\text{s}$ is comparable to interpretive χ_e^{exp} that reduces T_e gradient there to level which stabilizes P-B modes, suppresses ELMs,

  2) variation of $n_{e\,\text{ped}}$ (i.e., density pump-out) in Fig. 1 is qualitatively consistent with $D_{et}^{\text{flutt}}(t) \propto B_{mn}(t)^2$.

RMP ELM Suppression Issues Are Different In This Model

- Significant penetration of RMP to 8/2 surface is not caused by making $\Omega_e^\alpha \simeq \omega_{\perp e} \to \omega_E$ small there, but instead by an ELM crash.

- ELM crash produces strong FMR effects at 8/2 surface in ~ 1 ms:

  1) significant reconnection and magnitude of tearing-type response $\delta \mathrm{B}_\theta$,

  2) locking of $\delta \mathrm{B}_\theta$ to the stationary RMP (lab) frame by forcing $\omega_E \propto E_\rho \to 0$,

  3) a seed island whose further evolution is governed by nonlinear MRE.

- Bifurcation into ELM suppression is determined by nonlinear modified Rutherford equation (MRE) for 8/2 island evolution:

  1) applied RMP must be large enough for $\mathrm{w_{vac}} > \mathrm{w_{vac}^{crit}}$ so $\dot{\mathrm{w}} > 0$ is possible, which is favorable for ITER because $\mathrm{w_{vac}^{crit}}/a \propto \varrho_{*i}$ implies $B_{mn}^{\mathrm{vac}}/B_{\mathrm{t0}} \propto \varrho_{*i}^2$;

  2) ELM-crash-induced seed island must satisfy $\mathrm{w_{seed}} > \mathrm{w_{min}}$ for island growth.

- Analysis is for DIII-D discharge 158115.[1,2] More tests are needed to validate this new ELM-crash-induced ELM suppression model.

CEMM Can Contribute A Lot To These FMR Studies

- **NIMROD–M3D-C^1 cylindrical benchmarking is underway:**

  M. Beidler CEMM talk at 2:45 p and poster GP10.00076 on Tues. morning.

- **Next steps for NIMROD–M3D-C^1 benchmarking might focus on:**

  cylindrical: nonlinear evolution into island state, response to abrupt MHD;

  toroidal: linear RMP flow screening, drives; nonlinear evolution for FEs, $\cdots$.

- **Some issues for which procedures need to be developed and used:**

  1) RMP-drive parameter $\rho_{m/n}\Delta'_{\mathrm{RMP}\,m/n} \propto \overline{\delta J_{\parallel\,m/n}}$ — for cylinder & full torus,

  2) flutter transport effects on n_e and T_e in reconnection layer $\delta_\eta \simeq 0.14$ cm, which are already included via FMR torques and parallel heat conduction,

  3) poloidal and then toroidal torque balance and evolution of flows,

  4) inclusion of ion polarization current effects induced by $\vec{B}\times\vec{\nabla}\cdot\overleftrightarrow{\pi}_i$,

  5) *abrupt MHD perturbation (e.g., ELM) to jump into Rutherford regime,

  6) faster procedures for obtaining island growth in nonlinear MRE regime,

  7) unified MHD, kinetic, transport modeling via Chapman-Enskog approach.

Some Perspectives On Possible CEMM Future Thrusts

- **Forced magnetic reconnection studies may be fundamental to understanding many disruptions — because ELMs & sawteeth often initiate NTMs and facilitate penetration of resonant 3-D fields.**

- **Long term future of extended MHD studies likely involves unification of extended MHD, kinetic and transport models — so Chapman-Enskog-type kinetic equation is appropriate and could be solved using continuum or particle approach, or both.**

- **The present programmatic emphasis on simultaneous low torque (toroidal flow), high β and low q_{95} for ITER require careful integrated modeling of entire tokamak plasma environment — and would benefit from faster M3D-C^1 and NIMROD simulations.**

- **Even more comparisons of M3D-C^1 and NIMROD simulations with both experimental results <u>and</u> analytic theory for understanding are needed — but both are very time consuming and not adequately appreciated or supported.**